NUMERICAL SIMULATION OF NATURAL CONVECTION PHENOMENA

Santiago F. Corzo[a], Santiago Márquez Damián[a], Damian Ramajo[a] and Norberto M. Nigro[a]

[a]*International Center for Computational Methods in Engineering (CIMEC), INTEC-UNL/CONICET, Güemes 3450, Santa Fe, Argentina, santiagofcorzo@gmail.com, http://www.cimec.org.ar*

Keywords: Natural Convection, Finite Volume Method, Benchmark Solution, OpenFOAM®.

Abstract.

Natural convection heat transfer associated to fluid-dynamics phenomena has been extensively studied in many applications of scientific and industrial areas. Numerous benchmarks provide numerical and experimental data of these phenomena in a wide range of Rayleigh (Ra) numbers.

Three dimensional high Ra number regimes are particularly challenging to simulate due to instabilites sensitivity, need of correction of turbulence modeling and so on. The literature on this topic is scarce. In this paper Fluent and OpenFOAM codes have been used to assess the Boussinesq approximation for a wide range of Ra numbers ($10^3 - 10^8$) for two dimensional (square cavity) and three dimensional (cubic cavity) cases. High Ra number cases are particularly discussed showing model limitations and code capabilities to cope the natural convection phenomena. Results are compared with classical benchmark cases available in the literature, finding excellent agreement with both experimental and numerical data. Underlying theoretical models and implementantion are explained in depth, particularly for OpenFOAM code serving as a reference.

1 INTRODUCTION

Natural convection in closed cavities is of great importance in many engineering and scientific applications such as energy transfer, boilers, nuclear reactor systems, energy storage devices among others

In this sense the buoyancy-driven flow is a reliable case to test and validate computer codes such as those used in this paper, specifically Fluent® and OpenFOAM®. Related to this kind of problems natural convection in geometrically simple cases is a very good start point for both experimental and theoretical studies (Ampofo and Karayiannis, 2003).

The thermally driven flow in square cavity with adiabatic top and bottom walls is one of the classical problems in the heat transfer literature. It is used to test the numerical algorithms designed for the integration of the Navier-Stokes equations in incompresible recirculating flows (Le Quéré, 1991). This phenomenon has received considerable attention in numerical simulation due to the complexity of the problem relies on the strong coupling between the continuity and thermal equations at high Ra numbers.

Related to natural convection in closed cavities, both in laminar and turbulent regimes, there are two significant benchmark problems, the two-dimensional numerical solution given by De Vahl Davis (De Vahl Davis, 1983) and its three dimensional counterpart with experimental results taken from Ampofo et al (Ampofo and Karayiannis, 2003). Regarding the former tt has a set of numerical results for four values of Rayleigh number, namely 10^3, 10^4, 10^5 and 10^6 that were obtained with second-order central diference aproximation in a square cavity filled with air ($Pr = 0.71$) in laminar regime.

Although natural convection in enclosures has been extensively studied by several researchers (Patterson and Imberger, 1980) (Salat et al., 2004) (Dixit and Babu, 2006) both numerically and experimentally, there aren't many studies that provide results close to the critical Ra number where the flux becomes unsteady and close to physically unstable. This work contributes with a successful set of results at high Ra number (10^7 and 10^8) that could be used as a reference for future works. The agreement obtained with both codes allows to conclude that more complex thermal fluid dynamics problems may be analyzed with a reasonable accuracy. Moreover this paper may contribute as a reference for future validation of such a problems.

Regarding three dimensional cases, the experimental data for turbulent natural convection in a air filled cavity (0.75 m high × 0.75 m wide × 1.5 m deep) with a $Ra = 1.59 \times 10^9$ give worthy results at high Ra in terms of flux, thermal and turbulent quantities which are useful to compare with the results of turbulence models implemented in Fluent® and OpenFOAM®. In the last test the turbulence is modeled by means of LES Smagorinsky Model as proposed by Smagorinsky (Smagorinsky, 1963).

Several researchers had published their studies at low Reynolds turbulence regime in enclosures (Ampofo and Karayiannis, 2003), (Tian and Karayiannis, 2000) and (Peng and Davidson, 2000). As an extension, in this paper we present numerical results as good as those published earlier with the target put in applying such a solvers for more complex applications in the near future.

2 MATHEMATICAL FORMULATION

In natural convection problems the driven force is given by changes in fluid density due to temperature evolution. Even though the thermodynamical properties of the fluid are assumed to be constant, buoyancy body force term in the momentum equation are added allowing to relate density changes to temperature. This is achieved through the Boussinesq aproximation that couple the energy and the momentum equations. This aproximation is hold under certain hypothesis of small temperature differences.

The governing equations for newtonian incompresible fluid under laminar steady state flow can be written as in Equations 1-4:

$$\frac{\partial u}{\partial x} + \frac{\partial v}{\partial y} = 0 \tag{1}$$

$$u\frac{\partial u}{\partial x} + v\frac{\partial u}{\partial y} = -\frac{1}{\rho}\frac{\partial p}{\partial x} + \nu(\frac{\partial^2 u}{\partial x^2} + \frac{\partial^2 u}{\partial y^2}) \tag{2}$$

$$u\frac{\partial v}{\partial x} + v\frac{\partial v}{\partial y} = -\frac{1}{\rho}\frac{\partial p}{\partial y} + \nu(\frac{\partial^2 v}{\partial x^2} + \frac{\partial^2 v}{\partial y^2}) + F_b; \tag{3}$$

$$u\frac{\partial T}{\partial x} + v\frac{\partial T}{\partial y} = \alpha(\frac{\partial^2 T}{\partial x^2} + \frac{\partial^2 T}{\partial x^2}) \tag{4}$$

Under the hypothesis above mentioned the Boussinesq approximation can be written as in Equation 5 (Arpaci and Larsen, 1984).

$$F_b = g\beta(T - T_c) \tag{5}$$

With typical boundary conditions for the square (2D) cavity given by equations 6-9

$$u(x, 0) = u(x, L) = u(0, y) = u(L, y) = 0; \tag{6}$$

$$v(x, 0) = v(x, L) = v(0, y) = v(L, y) = 0; \tag{7}$$

$$T(0, y) = T_h; T(L, y) = T_c; \frac{\partial T}{\partial y}(x, 0) = \frac{\partial T}{\partial y}(x, L) = 0 \tag{8}$$

$$\frac{\partial T}{\partial y}(x, 0) = \frac{\partial T}{\partial y}(x, L) = 0 \tag{9}$$

here x and y are horizontal and vertical axis coordinate respectively; u and v are the velocity components in the x and y directions, T is the temperature, p the pressure and ρ the fluid density. Using nominal values given by Equations 10-11 a set of dimensionless governing equations can be derived (Equations 12 -15).

$$X = \frac{x}{H}; Y = \frac{y}{H}; U = \frac{uH}{\alpha}; V = \frac{vH}{\alpha}; \theta = \frac{T - T_c}{T_h - T_c}; \tag{10}$$

$$P = \frac{pL^2}{\rho\alpha^2}; Pr = \frac{\nu}{\alpha}; \tag{11}$$

$$\frac{\partial U}{\partial X} + \frac{\partial V}{\partial Y} = 0 \tag{12}$$

$$U\frac{\partial U}{\partial X} + V\frac{\partial U}{\partial Y} = -\frac{\partial P}{\partial X} + Pr(\frac{\partial^2 U}{\partial X^2} + \frac{\partial^2 U}{\partial Y^2}) \tag{13}$$

$$U\frac{\partial V}{\partial X} + V\frac{\partial V}{\partial Y} = -\frac{\partial P}{\partial Y} + Pr(\frac{\partial^2 V}{\partial X^2} + \frac{\partial^2 V}{\partial Y^2}) + RaPr\theta; \tag{14}$$

$$U\frac{\partial \theta}{\partial X} + V\frac{\partial \theta}{\partial Y} = (\frac{\partial^2 \theta}{\partial X^2} + \frac{\partial^2 \theta}{\partial X^2}) \tag{15}$$

with the non-dimensional boundary conditions given by equations 16-19.

$$U(X,0) = U(X,1) = U(0,Y) = U(1,Y) = 0; \tag{16}$$

$$V(X,0) = V(X,1) = V(0,Y) = V(1,Y) = 0; \tag{17}$$

$$\theta(0,Y) = 1; \theta(1,Y) = 0; \frac{\partial \theta}{\partial Y}(X,0) = \frac{\partial \theta}{\partial Y}(X,1) = 0 \tag{18}$$

$$\frac{\partial \theta}{\partial Y}(X,0) = \frac{\partial \theta}{\partial Y}(X,1) = 0 \tag{19}$$

Note in the above equations that U and V are Peclet numbers in the horizontal and vertical directions.

3 TWO DIMENSIONAL LAMINAR STEADY STATE MODEL IN SQUARE CAVITY

The problem presented deals with the two-dimensional flow of Prandtl number $Pr = 0.71$ in a square cavity of side H= 1m. The boundary conditions for the momentum equation are no slip at all boundaries. Horizontal walls are isolated, and the vertical sides are at diferent temperatures ($T_c < T < T_h$). This case allows to verify the limit in Ra number where the fluid configuration becomes unsteady. It was verified that this limit is very close to 2×10^8, which is the transition point widely studied by Paolucci and Chenoweth (Paolucci and Chenoweth, 1989) and by Le Quéré (Le Quéré, 1991). The main interest of this work is to give accurate solutions to Ra numbers from 10^7 to 10^8 and larger which result in non-trivial cases. Difficulties arise from the coupling between momentum and energy equations in the transition range of Reynolds number (Re) between laminar and turbulent regime. Remember that (Re) number is related to (Ra) number increasing monotonically as approximately a square root.

For simplicity all the tests were run changing the value of gravitational acceleration until obtain the right Ra number, keeping all the other variables constant. Figure 1 exhibits the geometry of the cavity.

Simulations were carried out using two grids of 100×100 and 200×200 cells respectively with refinement towards the walls. The refinement is controlled by the code needs as will be discussed below. The wide range of Ra (Equation 20) numbers was obtained by a constant
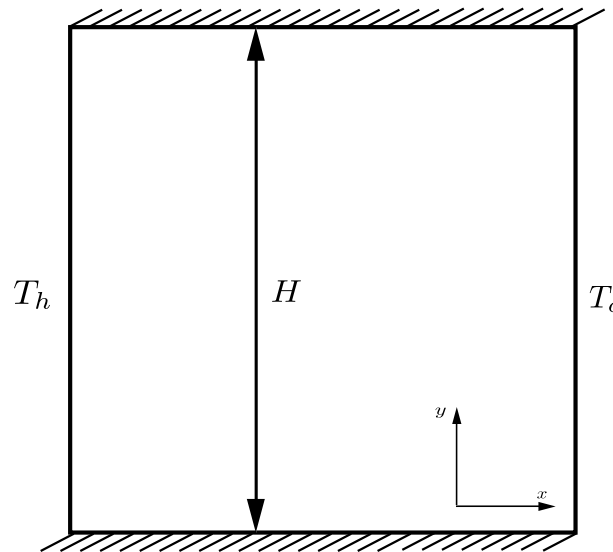
Figure 1: Detail of Cavity simulated, left wall at Th, right wall at Tc, front, back,top and bottom walls are insulated

temperature difference of $\Delta T = 1K$ adjusting the gravitational aceleration to supply the desired Ra .

$$Ra = \frac{g\beta L^3(T_h - T_c)}{\alpha\nu} \qquad (20)$$

where α is the thermal diffusivity and β the thermal expansion coefficient corresponding to air with $Pr = \nu/\alpha = 0.71$ in Standard Temperature and Pressure conditions.

3.1 Solvers settings

Fluent®   The case was set with a pressure based, segregated, steady solver with Green-Gauss Cell Based gradient treatment. SIMPLE algorithm was selected for the pressure-velocity coupling with relaxation factors of 0.3 for pressure, 0.7 for momentum and 1 for energy as the defaults. The pressure was discretized with Standard discretisation based on Rhie and Chow (Rhie and Chow, 1983) and QUICK was chosen for advection scheme for momentum and energy discretization.

The residual criteria of convergence were set for absolute residuals (Equation 21) below of 1×10^{-7} for all the variables in all the cases.

$$R^\phi = \frac{\sum_{\text{cells } P} |\sum_{\text{N}} a_{\text{N}}\phi_{\text{N}} + b - a_P\phi_P|}{\sum_{\text{cells } P} |a_P\phi_P|} \qquad (21)$$

being a_P the center coefficient[1], i.e. the contribution of all terms that involves the unknown at the cell center, a_{N} are the influence coefficients for the neighboring cells, namely the cells that share a face with the analyzed cell, and b is the contribution of the constant part of the source term S_c in $S = S_c + S_P\phi$ and of the boundary conditions.

---

[1]See Fluent® 6.3.26 Users Guide, chapter 25.18.1

OpenFOAM®   A pressure based, segregated, steady solver (`buoyantBoussinesq-SimpleFoam`) was used with SIMPLE algorithm for pressure-velocity coupling with relaxation factors of 0.3 for pressure, 0.7 for momentum and 1 for energy. Residuals were reduced below of 1×10^{-7} for all variables and Gauss QUICK discretisation was set for divergence terms. Regarding residuals criteria the definition are quite similar, so then similar criteria for convergence were set. OpenFOAM® residuals definition lies on scaled residuals theory too, nevertheless different scaling factor are used, an explanation was given by Jasak (See CFD On-line OpenFOAM® Convergence on Segregated Solvers thread) and Márquez Damián and Nigro (Márquez Damián and Nigro, 2010). The same formulation for the pressure discretisation as in Fluent was used and it was set by means of Gauss Linear scheme (Peng and Davidson, 2000).

3.2   Results and Discussion

This section is divided as follows: the first part provides a set of solutions at low Ra number and leaves the more interesting high Ra number case to be analyzed at the end of the section.

The quantities under study are the following:

- $[u_{max(1/2)}]$: The maximum horizontal velocity on the vertical mid-plane of the cavity (together with its location).

- $[v_{max(1/2)}]$: The maximum vertical velocity on the horizontal mid-plane of the cavity (together with its location).

- $[Nu_0]$: The average Nusselt number on the vertical boundary of the cavity at $x = 0$.

- $[Nu_{max}]$: The maximum value of the local Nusselt number on the boundary at $x = 0$ (together with its location).

- $[Nu_{min}]$: The minimun value of the local Nusselt number on the boundary at $x = 0$ (together with its location).

Tables 1-4 show both Fluent® and OpenFOAM® results for $Ra = 10^3$, 10^4, 10^5 and 10^6 compared with the De Vahl Davis (De Vahl Davis, 1983) solutions. Excellent agreement to experimental data in both results for momentum and energy quantities prove the accuracy of this approach for this low Ra number range. The horizontal velocity component in the vertical mid-plane is shown in Figure 2. Here is worthy to note that when Ra number increases the boundary layer becomes more defined and the maximum values in the velocity get closer to the walls.

The heat flux in the cavity is characterized for an ascendent movement in the hot wall and decendent one in the cold wall due to the buoyancy and gravitational acceleration respectively. In the low Ra cases the heat transfer is driven predominantly by conduction as seen in Figure 3 where the local Nusselt number takes small values. The Nusselt number was computed using the following expresion 22:

$$Nu = \frac{hL}{\kappa} \tag{22}$$

Table 1: Numerical Solution with Fluent® and OpenFOAM® codes

	Ra = 10^3				
	Fluent	OpenFOAM	G.V. Davis		
			h=0.1	h=0.05	h=0.025
$u_{max}(x = 0.5)$	3.643	3.640	3.427	3.589	3.634
$y_{max}(x = 0.5)$	0.817	0.812	0.801	0.811	0.813
$v_{max}(y = 0.5)$	3.690	3.700	3,449	3,629	3,679
$x_{max}(y = 0.5)$	0.182	0.177	0,193	0,181	0,179
Nu_0	1.113	1.109	1.105	1.113	1.116
$Nu_{max}(x = 0)$	1.506	1.505	1.462	1.491	1.501
$y_{max}(x = 0)$	0.090	0.001	0.141	0.112	0.087
$Nu_{min}(x = 0)$	0.691	0.691	0.723	0.702	0.694
$y_{min}(x = 0)$	1.000	1.000	0.936	1.000	1.000

Table 2: Numerical Solution with Fluent® and OpenFOAM® codes

	Ra = 10^4				
	Fluent	OpenFOAM	G.V. Davis		
			h=0.1	h=0.05	h=0.025
$u_{max}(x = 0.5)$	16.139	16.281	16.243	16.189	16.182
$y_{max}(x = 0.5)$	0.817	0.822	0.808	0.820	0.823
$v_{max}(y = 0.5)$	19.619	19.547	18.055	19,197	19,509
$x_{max}(y = 0.5)$	0.119	0.123	0.139	0.125	0.120
Nu_0	2.246	2.222	2.307	2.255	2.242
$Nu_{max}(x = 0)$	3.539	3.538	3.637	3.603	3.545
$y_{max}(x = 0)$	0.144	0.085	0.211	0.165	0.149
$Nu_{min}(x = 0)$	0.691	0.691	0.676	0.610	0.592
$y_{min}(x = 0)$	1.000	1.000	1.000	1.000	1.000

Table 3: Numerical Solution with Fluent® and OpenFOAM® codes

	Fluent	OpenFOAM	G.V. Davis				
Ra = 10^5							
			h=0.1	h=0.05	h=0.025	h=0.016	h=0.0125
$u_{max}(x=0.5)$	34.469	34.928	40.900	36.460	35.070	34.870	34.810
$y_{max}(x=0.5)$	0.855	0.859	0.846	0.854	0.855	0.855	0.855
$v_{max}(y=0.5)$	68.817	68.878	59.710	62.790	66.730	67.910	68.220
$x_{max}(y=0.5)$	0.064	0.067	0.083	0.075	0.068	0.067	0.066
Nu_0	4.535	4.498	4.767	4.716	4.564	4.531	4.523
$Nu_{max}(x=0)$	7.767	7.765	6.538	7.901	7.905	7.802	7.761
$y_{max}(x=0)$	0.083	0.080	0.218	0.133	0.095	0.087	0.085
$Nu_{min}(x=0)$	0.691	0.726	1.516	0.797	0.755	0.741	0.736
$y_{min}(x=0)$	1.000	1.000	1.000	0.973	1.000	1.000	1.000

Table 4: Numerical Solution with Fluent® and OpenFOAM® codes

|	Fluent	OpenFOAM	G.V. Davis				
Ra = 10^6							
			h=0.1	h=0.05	h=0.025	h=0.016	h=0.0125
$u_{max}(x=0.5)$	64.433	64.558	230.22	79.27	67.49	65.81	65.33
$y_{max}(x=0.5)$	0.846	0.851	0.915	0.862	0.854	0.852	0.851
$v_{max}(y=0.5)$	220.970	221.572	213.91	195.44	206.32	214.64	216.75
$x_{max}(y=0.5)$	0.0379	0.0670	0.0670	0.0447	0.0423	0.0396	0.0387
Nu_0	8.861	8.786	6.790	9.502	9.270	9.035	8.928
$Nu_{max}(x=0)$	17.717	17.708	7.959	14.215	17.947	18.255	18.076
$y_{max}(x=0)$	0.0379	0.0404	0.138	0.124	0.0675	0.0523	0.0456
$Nu_{min}(x=0)$	0.983	0.977	3.853	1.749	1.015	1.020	1.005
$y_{min}(x=0)$	1.000	0.998	1.000	1.000	0.984	1.000	1.000
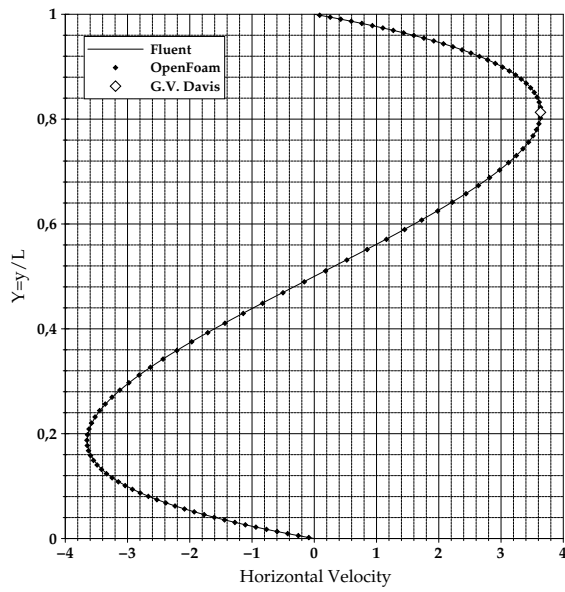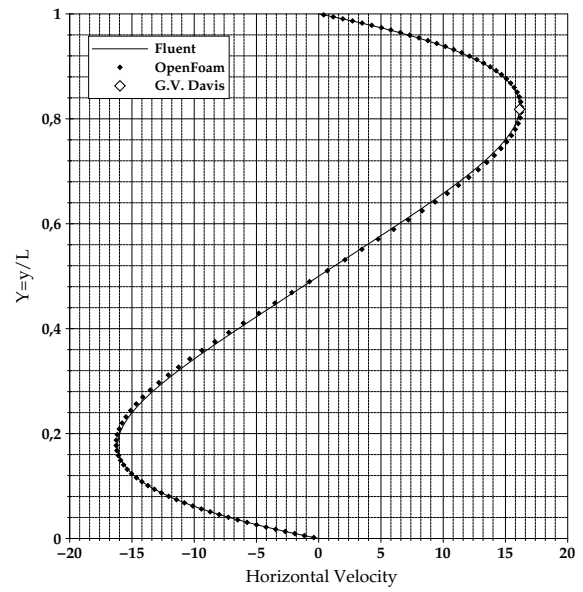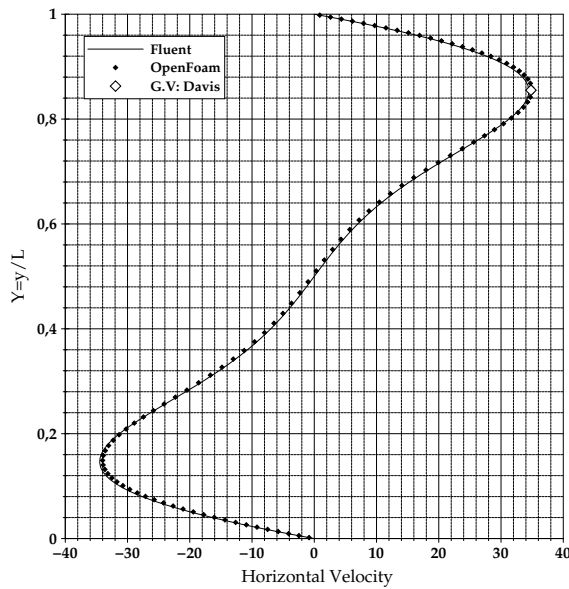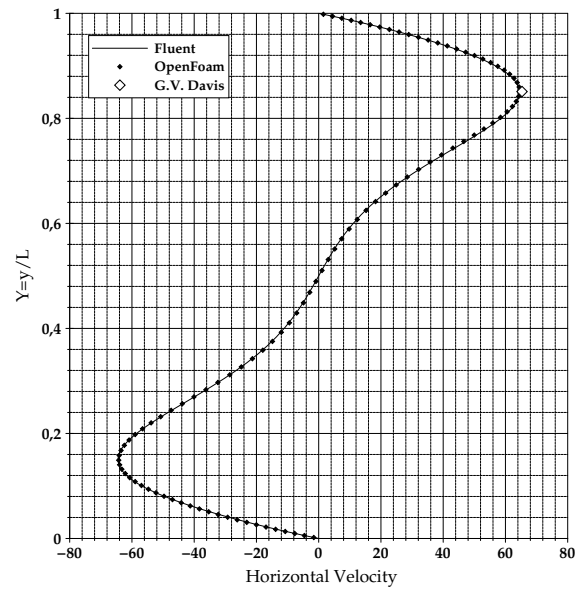
Figure 2: Horizontal velocity profiles ($U = u/\alpha$) at x mid-plane to a) $Ra = 10^3$, b) $Ra = 10^4$, c) $Ra = 10^5$ and d) $Ra = 10^6$
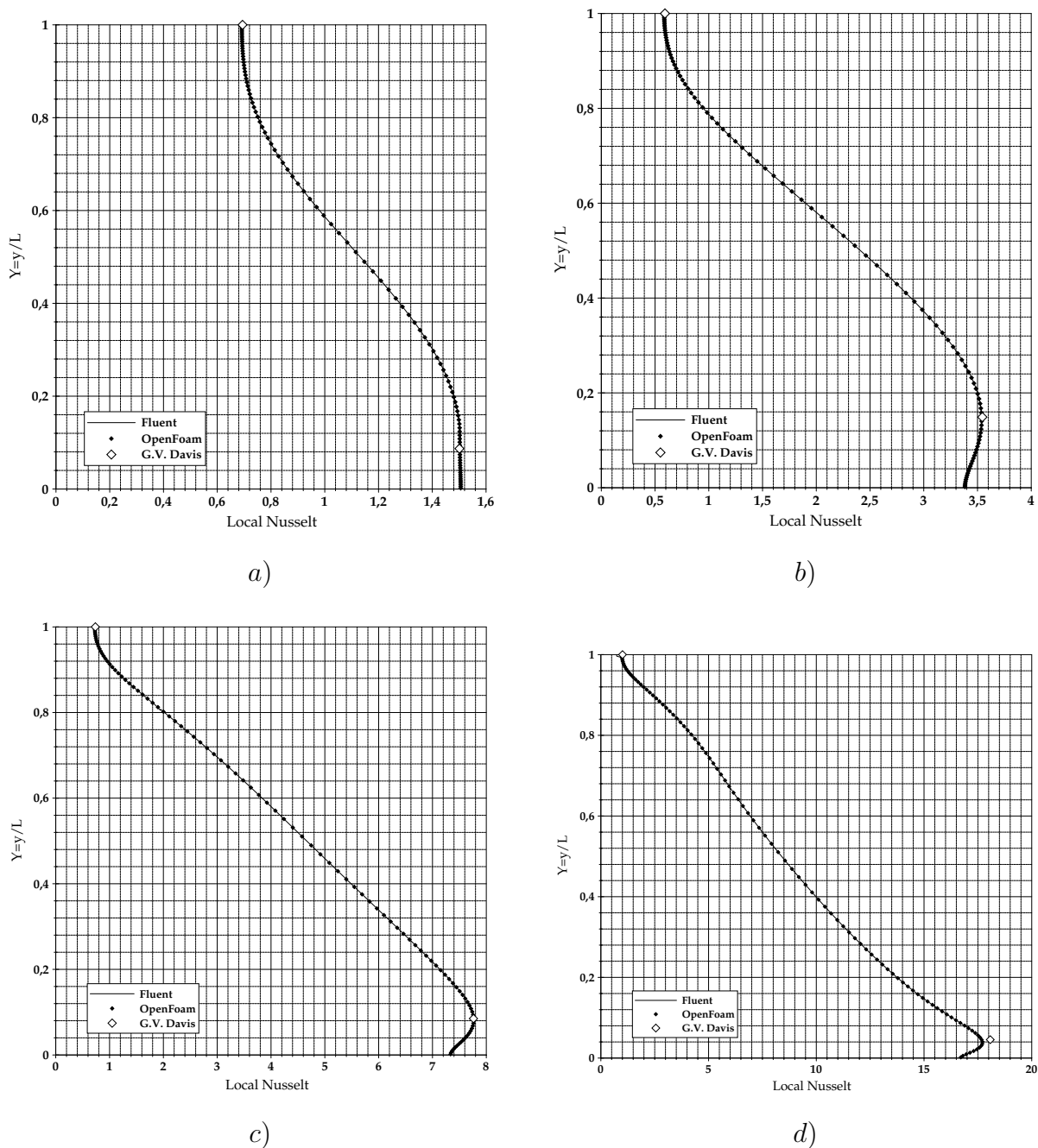
Figure 3: Local Nusselt on the hot wall at a) $Ra = 10^3$, b) $Ra = 10^4$, c) $Ra = 10^5$ and d) $Ra = 10^6$
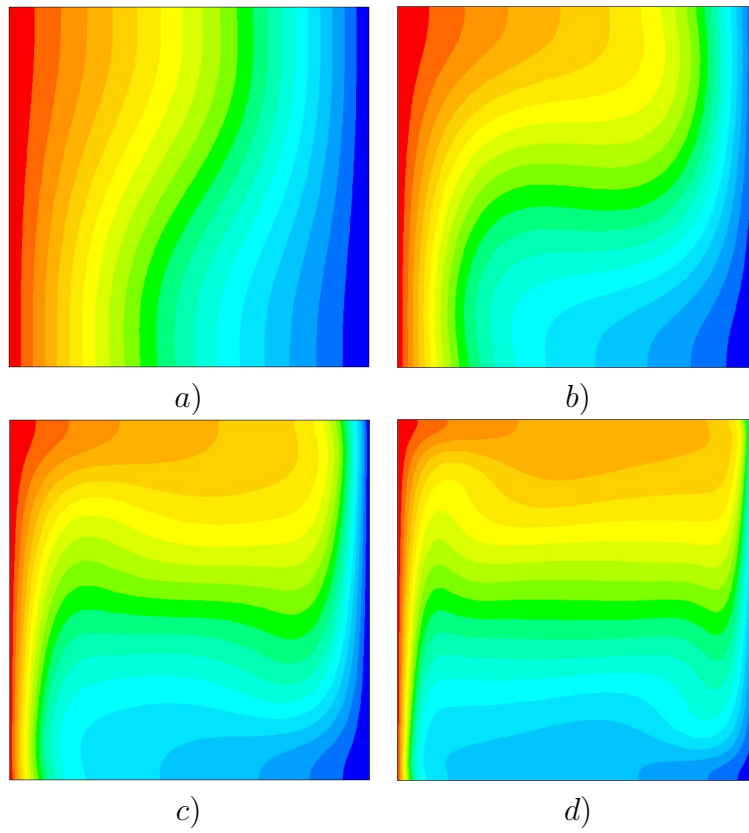
Figure 4: Temperature field $\theta = \frac{T-T_c}{T_h-T_c}(0-1)$ to a) $Ra = 10^3$, b) $Ra = 10^4$, c) $Ra = 10^5$ and d) $Ra = 10^6$

where h is the convective heat transfer coefficient on the wall and κ is the thermal conductivity of the fluid. Finally Figure 4 gives the temperature profiles for the four cases.

Related to high Ra number tests, steady state results from both codes show excellent agreement and may be used as a reference for coupled equation simulation. Due to the difficulties in obtaining a converged solution at the beginning of this study, results from previous tests were used as an initial guess for the higher Rayleigh number cases. First-order divergence scheme was used as well. Once first-order solution was obtained the calculation was continued using QUICK interpolation scheme. For the last two-dimentional test ($Ra = 10^8$) performed in OpenFOAM® it was necesary to refine the grid (200×200 cells) in order to obtain an accurate solution with the same residual criteria.

Table 5: Numerical Solution with Fluent® and OpenFOAM® codes

	Fluent	OpenFOAM	P. Le Quéré
Ra = 10^7			
			h=1/80
$u_{max}(x = 0.5)$	146.00	145.84	148.58
$y_{max}(x = 0.5)$	0.888	0.884	0.879
$v_{max}(y = 0.5)$	695.36	704.094	699.236
$x_{max}(y = 0.5)$	0.0196	0.0217	0.021
Nu_0	16.645	16.502	16.523
$Nu_{max}(x = 0)$	40.619	40.594	39.39
$y_{max}(x = 0)$	0.015	0.017	0.018
$Nu_{min}(x = 0)$	1.394	1.365	1.366
$y_{min}(x = 0)$	0.990	0.998	1.000

Table 6: Numerical Solution with Fluent® and OpenFOAM® codes

	Fluent	OpenFOAM	P. Le Quéré
Ra = 10^8			
			h=1/128
$u_{max}(x = 0.5)$	304.015	299.156	321.876
$y_{max}(x = 0.5)$	0.922	0.921	0.928
$v_{max}(y = 0.5)$	2199.51	2233.35	2222.39
$x_{max}(y = 0.5)$	0.011	0.012	0.012
Nu_0	28.52	30.1425	30.225
$Nu_{max}(x = 0)$	96.47	90.294	87.24
$y_{max}(x = 0)$	0.0074	0.008	0.008
$Nu_{min}(x = 0)$	2.0536	1.906	1.919
$y_{min}(x = 0)$	0.999	0.999	1.000

Figure 5 shows the horizontal velocity profile in the vertical mid-line. These results exhibit good agreement between both softwares and with benchmark results as shown in the tables 5, 6. The flow is limited to a narrow strip along the wall where the velocity and temperture change suddenly.
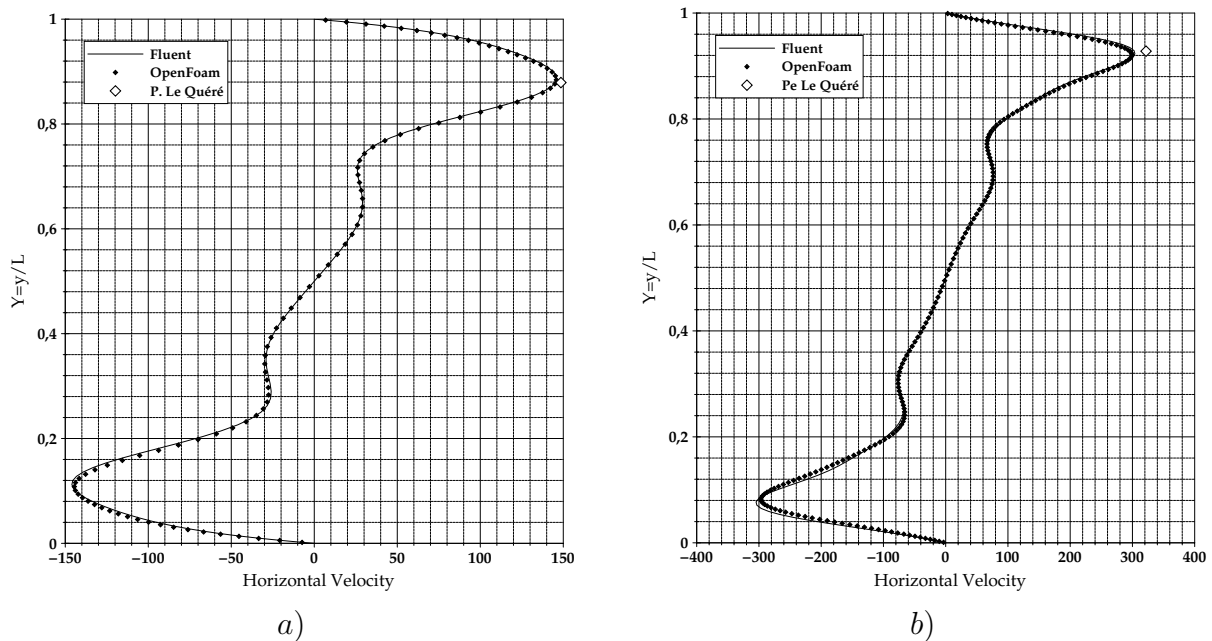

Figure 5: Horizontal velocity profiles ($u = U/\alpha$) at x mid-plane to a) Ra = 10^7 and b) Ra = 10^8

The local Nu on the hot wall of the cavity is shown in Figure 6. It reaches its maximum at the bottom of the hot wall because of the thinner thermal boundary layer presented there. As the thickness of the boundary increases along the flow direction, the local Nu drecreases rapidly.

4 TURBULENT NATURAL CONVECTION IN AN THREE DIMENSIONAL CAVITY

The problem to be solved is a test rig of natural convection in a enclosure domain. The cavity was 0.75m high $\times\, 0.75$m wide $\times\, 1.5$m deep, see Figure 8. The hot wall was kept at $50\pm0.15\,^\circ$C whilst the cold wall at $10 \pm 0.15\,^\circ$C giving a $Ra = 1.59 \times 10^9$. The horizontal walls were kept isolated.

The publication of this three-dimensional test (Ampofo and Karayiannis, 2003; Tian and Karayiannis, 2000) includes several experimental results that allow to do a good estimation of turbulence quantities. Here we study only mean transport variables and thermal properties leaving the turbulent correlations for future works.

4.1 Solvers settings

Fluent®   The case was set as in Fluent® 2D model with a pressure based, segregated, unsteady implicit Crank-Nickolson formulation with Green-Gauss Cell Based gradient treatment. PISO
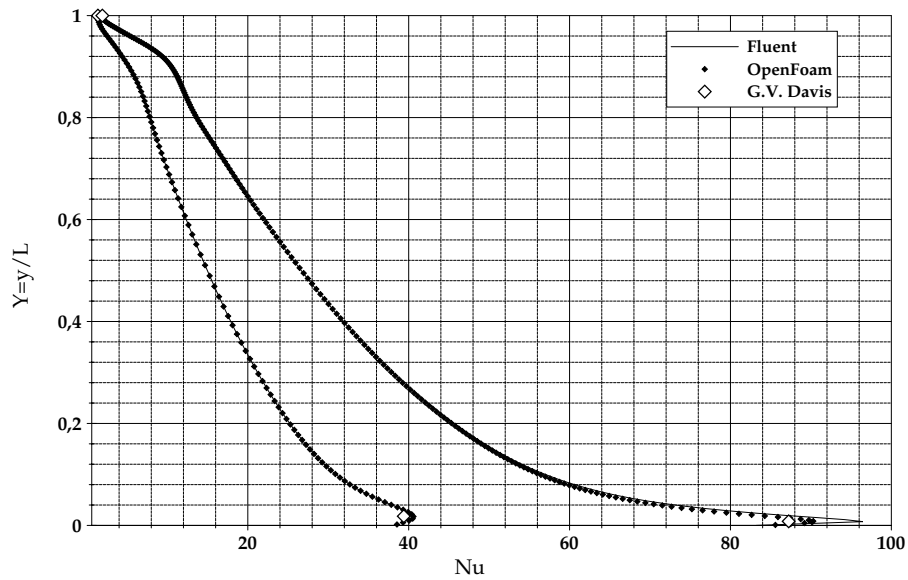
Figure 6: Local Nusselt on the hot wall at Ra = 10^7 and Ra = 10^8
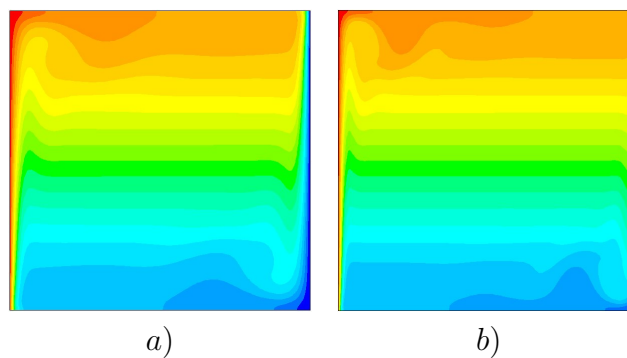

$a)$ $b)$

Figure 7: Temperature field $\theta = \frac{T-T_c}{T_h-T_c}(0-1)$ to a) $Ra = 10^7$ and b) $Ra = 10^8$
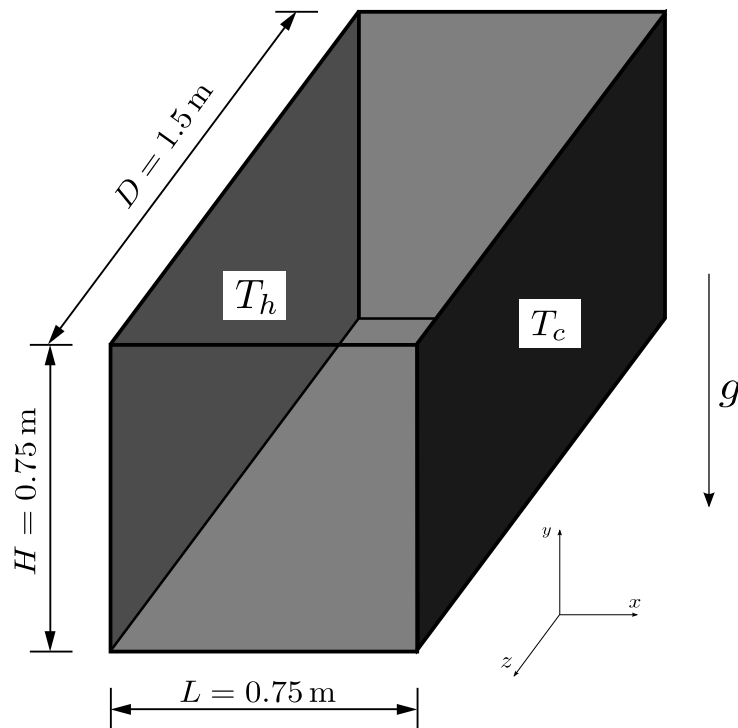
Figure 8: Detail of Cavity simulated

algorithm was selected for pressure-velocity coupling with relaxation factors of 0.3 for pressure, 0.7 for momentum and 1 for energy. The pressure was discretized with Standard discretisation and Second order Upwind was set for momentum and energy discretisation equation. The residuals criteria of convergence was such that reduce the absolute residuals below of 1×10^{-5} for all the variables in all the cases. The turbulence was modeled using Large Eddy Simulation (LES) taking into account previous work (Peng and Davidson, 2000). Static Smagorisky was chosen as the subgrid scale model (SGS).

OpenFOAM® Like in Fluent® a pressure based, segregated, steady state solver (`buoyant-BoussinesqPisoFoam`) with PISO algorithm for pressure-velocity coupling was selected. Gauss second order upwind discretization was set for pressure and divergence terms. Residuals were reduced below of 1×10^{-5} for all variables. LES was used to simulate the turbulence with Static Smagorisky model to estimate the subgrid-scale stresses. The same constants as in Fluent® code were selected.

4.2 Results and Discussion

Several works (Penot and Ndame, 1993; Tian and Karayiannis, 2000) pointed out that the 2D approximation of experimental natural convection in cavities should be valid only if the horizontal aspect ratio (AR) of the cavity is greater than 1.8. The cavity modeled in this paper has an AR=2, hence, for this reason the mid-section cavity has a two-dimentional behavior and so these results are reported. It is worthy to note that this assumption is not easely achieved.

Owe to the non-steady character of the flux time-averaged value of all solution variables in the mid-line ($Y = 0.5$, $Z = 0, 5$) and the Nu number in wall line ($X = 0$, $Z = 0, 5$) are

reported. The mean quantities $(\overline{u}, \overline{v}, \overline{T})$ were computed by means of Equation 23.

$$\overline{m} = \frac{1}{N} \sum_i m_i \tag{23}$$

Both Fluent® and OpenFOAM® were set to take averages of the transport variables in each time step. Statistics started when stationary state was achieved. The number of time steps averaged N was chosen with the aim to complete a full cycle in the vertical velocity variation over the mid-line.

Figure 9 and 10 shows the mean vertical velocity in the mid-plane and the temperature distribution at the same points. Even though the comparison between numerical and experimental velocity and temperature profiles reveals discrepancies, the accuracy of the two results presented in this paper is suitable to be compared with other numerical results cited in the bibliography. Probably one of the main reasons of this discrepancy could be the adiabatic boundary condition in the horizontal walls (Tian and Karayiannis, 2000). This boundary condition is experimentally very hard to set up, specially in air filled enclosures.

The high Ra number give a thin boundary layer where the fluid is dragged by the buoyant and gravitational effects. Velocity and thermal profiles have a good agreement despite of the coarse mesh close to the wall employed. The flow is characterized by low Reynolds turbulence intensity and thermal stratification. From $X = 0.08$ to $X = 0.92$, the temperature holds approximately constant, indicating that the fluid in the core area is nearly stagnant.
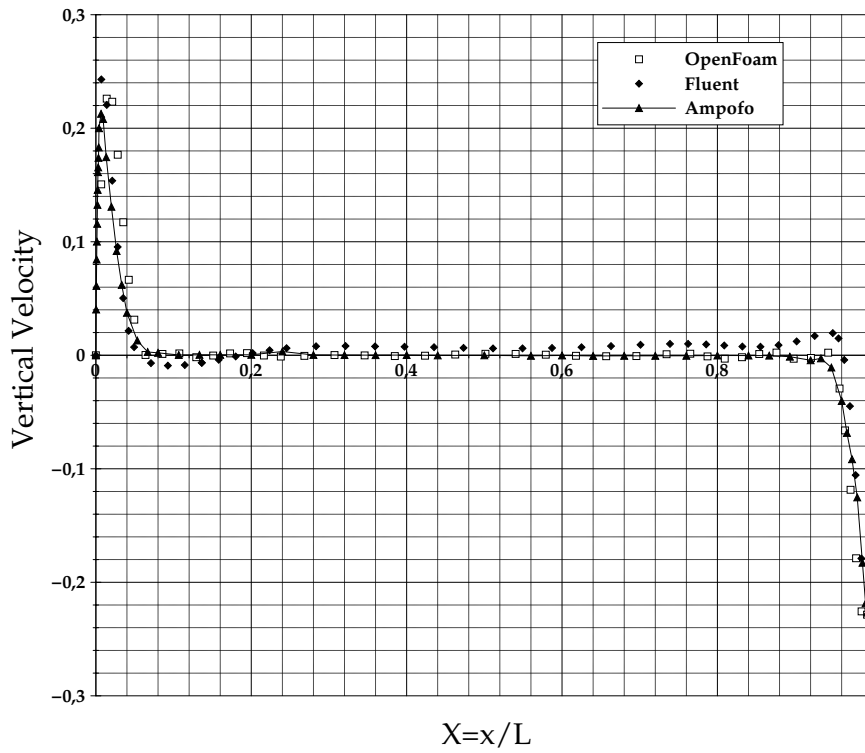
a)
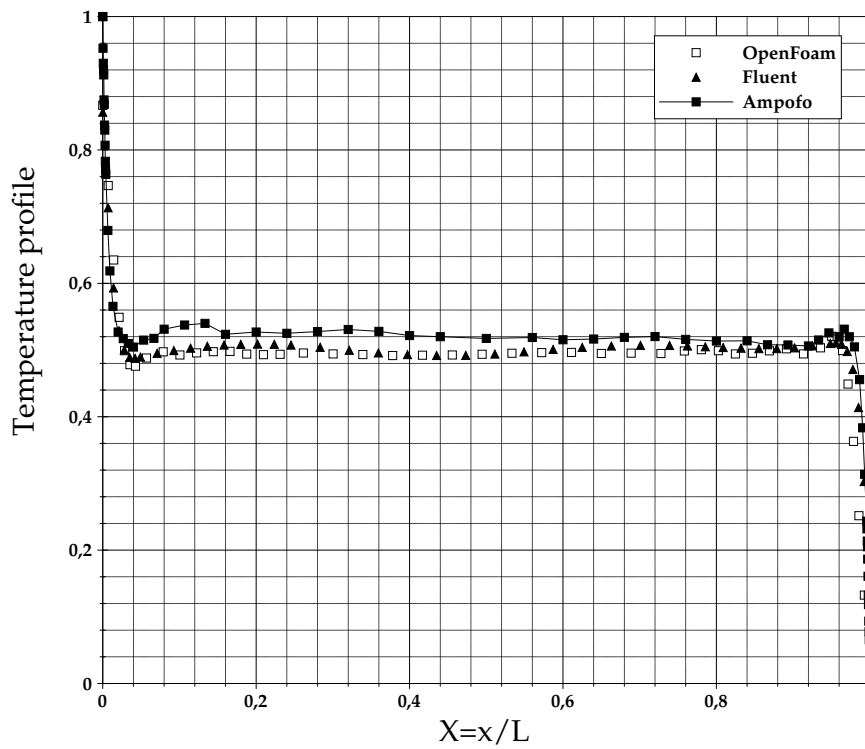
b)

Figure 9: Mid-plane ($Y = 0.5$, $Z = 0,5$) transport properties: a) Vertical velocity profiles ($v = V/Vo$) and b) Temperature field $\theta = \frac{T-T_c}{T_h-T_c}$
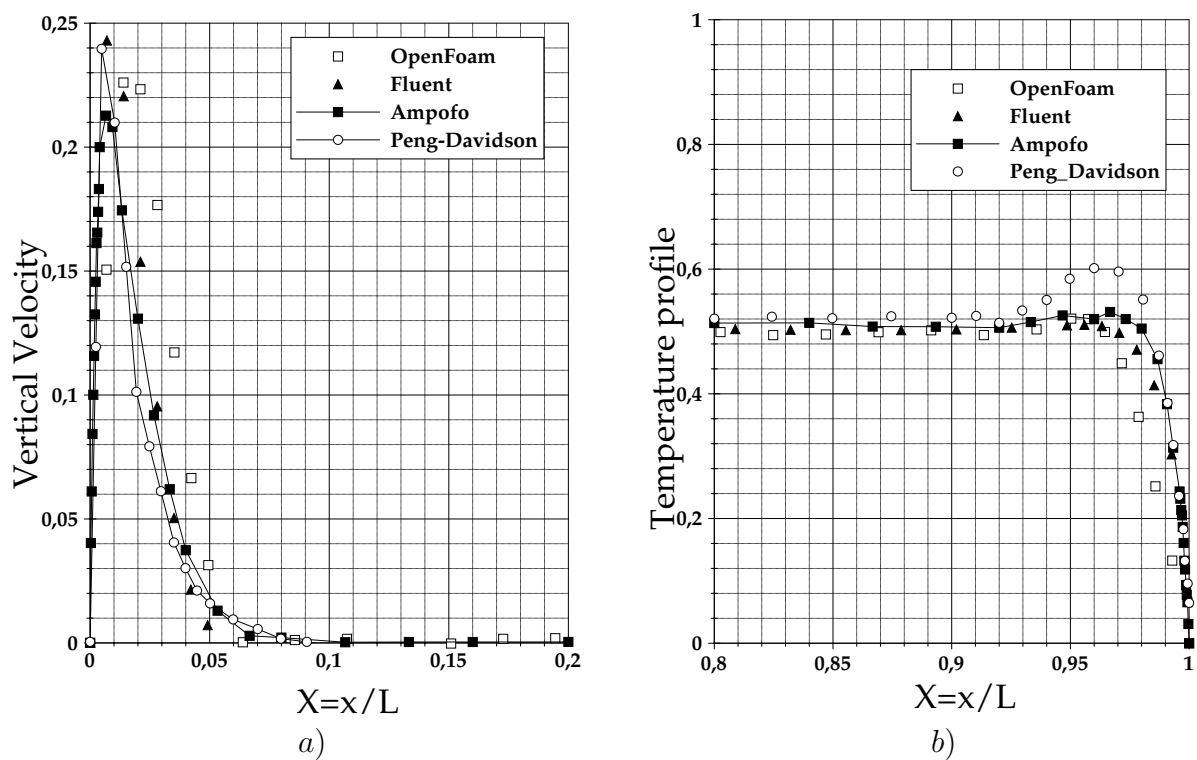
Figure 10: Mid-plane ($Y = 0.5$, $Z = 0, 5$) transport properties: a) Vertical velocity profiles ($v = V/Vo$) and b) Temperature field $\theta = \frac{T - T_c}{T_h - T_c}$

5 CONCLUSIONS

The results presented in this paper reveals a good agreement not only in 2D also in 3D and for a wide range of Ra numbers. In this sense they can be set as a reference for future buoyancy-driven tests. In addition the usage of a free software code as OpenFOAM® and its comparison against a very well known software as Fluent has been another purpose of the present work. We prove that it is possible to solve the strong coupling between energy and momentum equations produced at high Rayleigh numbers. Finally the preliminar 3D results for low Reynolds turbulence regime seems to be very promissory specially due to the reasonable good accuracy obtained from the mean values. Probably more work is needed to tune other turbulence quantities before using such a models in more complex applications like those found in nuclear power plants.

REFERENCES

Ampofo F. and Karayiannis T. Experimental benchmark data for turbulent natural convection in an air filled square cavity. *International Journal of Heat and Mass Transfer*, 46(19):3551–3572, 2003.

Arpaci V. and Larsen P. *Convection Heat Transfer*. Prentice-Hall, 1984.

De Vahl Davis G. Natural convection of air in a square cavity: a bench mark numerical solution. *International Journal for Numerical Methods in Fluids*, 3(3):249–264, 1983.

Dixit H. and Babu V. Simulation of high rayleigh number natural convection in a square cavity using the lattice boltzmann method. *International journal of heat and mass transfer*, 49(3-4):727–739, 2006.

Le Quéré P. Accurate solutions to the square thermally driven cavity at high rayleigh number. *Computers & Fluids*, 20(1):29–41, 1991.

Márquez Damián S. and Nigro N.M. Comparison of Single Phase Laminar and Large Eddy Simulation (LES) Solvers Using the OpenFOAM Suite. In *Mecánica Computacional Vol XXIX (2010)*, pages 3721–3740. 2010.

Paolucci S. and Chenoweth D. Transition to chaos in a differentially heated vertical cavity. *J. Fluid Mech*, 201:379–410, 1989.

Patterson J. and Imberger J. Unsteady natural convection in a rectangular cavity. *J. Fluid Mech*, 100(1):65–86, 1980.

Peng S. and Davidson L. Numerical investigation of turbulent buoyant cavity flow using large eddy simulation. In *Int. Symp. Turbulence Heat Mass Transfer*, volume 3, pages 737–744. 2000.

Penot F. and Ndame A. Successive bifurcations of natural convection in a vertical enclosure heated from the side. In *Institution Of Chemical Engineers Symposium Series*, volume 129, pages 507–507. Hemsphere Publishing Corporation, 1993.

Rhie C. and Chow W. Numerical study of the turbulent flow past an airfoil with trailing edge separation. *AIAA*, 21, 1983.

Salat J., Xin S., Joubert P., Sergent A., Penot F., and Le Quere P. Experimental and numerical investigation of turbulent natural convection in a large air-filled cavity. *International journal of heat and fluid flow*, 25(5):824–832, 2004.

Smagorinsky J. General circulation experiments with the primitive equations. 1.the basic experiment. *Mon. Weather Rev.*, 91:99–164, 1963.

Tian Y. and Karayiannis T. Low turbulence natural convection in an air filled square cavity:: Part i: the thermal and fluid flow fields. *International Journal of Heat and Mass transfer*,

43(6):849–866, 2000.